ORIGINAL RESEARCH

Myocardial Blood Flow Quantification Using Stress Cardiac Magnetic Resonance Improves Detection of Coronary Artery Disease

Shuo Wang, MD,[a] Paul Kim, MD,[b] Haonan Wang, PhD,[c] Ming-Yen Ng, BMBS,[d] Andrew E. Arai, MD,[e] Amita Singh, MD,[f] Saima Mushtaq, MD,[g] Tsun Hei Sin, BSc,[d] Yuko Tada, MD, PhD,[b] Elizabeth Hillier, MD, PhD,[h,i] Ruyun Jin, MD, MCR,[j] Christian Østergaard Mariager, PhD,[k] Michael Salerno, MD, PhD,[l] Gianluca Pontone, MD,[g,m] Javier Urmeneta Ulloa, PhD,[n] Ibrahim M. Saeed, MD,[o,p] Hena Patel, MD,[q] Victor Goh, MBBS,[r] Simon Madsen, MD,[k] Won Yong Kim, MD,[s] Mayil Singram Krishnam, MD,[t] Vicente Martínez de Vega, MD,[n] Alicia M. Maceira, MD, PhD,[u] Jose V. Monmeneu, MD, PhD,[u] Aju P. Pazhenkottil, MD,[v] Alborz Amir-Khalili, PhD,[w] Mitchel Benovoy, PhD,[x] Silke Friedrich, MD,[x] Martin A. Janich, PhD,[y] Matthias G. Friedrich, MD,[h,z] Amit R. Patel, MD[a]

ABSTRACT

BACKGROUND Myocardial blood flow (MBF) and myocardial perfusion reserve (MPR) using stress cardiovascular magnetic resonance (CMR) have been shown to identify epicardial coronary artery disease. However, comparative analysis between quantitative perfusion and conventional qualitative assessment (QA) remains limited.

OBJECTIVES The aim of this multicenter study was to test the hypothesis that quantitative stress MBF (sMBF) and MPR analysis can identify obstructive coronary artery disease (obCAD) with comparable performance as QA of stress CMR performed by experienced physicians in interpretation.

METHODS The analysis included 127 individuals (mean age 62 ± 16 years, 84 men [67%]) who underwent stress CMR. obCAD was defined as the presence of stenosis ≥50% in the left main coronary artery or ≥70% in a major vessel. Each patient, coronary territory, and myocardial segment was categorized as having either obCAD or no obCAD (noCAD). Global, per coronary territory, and segmental MBF and MPR values were calculated. QA was performed by 4 CMR experts.

RESULTS At the patient level, global sMBF and MPR were significantly lower in subjects with obCAD than in those with noCAD, with median values of sMBF of 1.5 mL/g/min (Q1-Q3: 1.2-1.8 mL/g/min) vs 2.4 mL/g/min (Q1-Q3: 2.1-2.7 mL/g/min) ($P < 0.001$) and median values of MPR of 1.3 (Q1-Q3: 1.0-1.6) vs 2.1 (Q1-Q3: 1.6-2.7) ($P < 0.001$). At the coronary artery level, sMBF and MPR were also significantly lower in vessels with obCAD compared with those with noCAD. Global sMBF and MPR had areas under the curve (AUCs) of 0.90 (95% CI: 0.84-0.96) and 0.86 (95% CI: 0.80-0.93). The AUCs for QA by 4 physicians ranged between 0.69 and 0.88. The AUC for global sMBF and MPR was significantly better than the average AUC for QA.

CONCLUSIONS This study demonstrates that sMBF and MPR using dual-sequence stress CMR can identify obCAD more accurately than qualitative analysis by experienced CMR readers. (JACC Cardiovasc Imaging. 2024;■:■-■)
© 2024 The Authors. Published by Elsevier on behalf of the American College of Cardiology Foundation. This is an open access article under the CC BY-NC-ND license (http://creativecommons.org/licenses/by-nc-nd/4.0/).

ABBREVIATIONS AND ACRONYMS

AIF = arterial input function

CAD = coronary artery disease

CMR = cardiac magnetic resonance

CTA = computed tomographic angiography

ICA = invasive coronary angiography

LGE = late gadolinium enhancement

MBF = myocardial blood flow

MPR = myocardial perfusion reserve

noCAD = no obstructive coronary artery disease

obCAD = obstructive coronary artery disease

QA = qualitative assessment

QP = quantitative perfusion

rMBF = rest myocardial blood flow

sMBF = stress myocardial blood flow

Stress cardiac magnetic resonance (CMR) is now recommended for the assessment of coronary artery disease (CAD) in both the American College of Cardiology/American Heart Association and European Society of Cardiology guidelines, which underscores the ability of the modality to accurately and cost-effectively assess ischemia, cardiac function, and viability;[1,2] identify those in need of revascularization;[3] and provide clinical prognostic value.[4] Nonetheless, stress CMR remains underused, in part because of its limited availability.[4,5]

Recent advances in stress CMR allow the quantification of global and segmental myocardial blood flow (MBF) in units of milliliters per gram per minute and myocardial perfusion reserve (MPR). The quantification of MBF and MPR has the potential to improve the detection of both epicardial and microvascular coronary abnormalities.[6,7] However, it remains less clear whether quantitative perfusion (QP) improves the diagnostic accuracy of stress CMR for obstructive coronary artery disease (obCAD) in comparison with qualitative assessment (QA), as currently published studies have produced inconsistent findings.[8-10] In this study, we used a dual-sequence, first-pass CMR approach,[6] which modifies a traditional perfusion sequence to include both arterial input function (AIF) and myocardial information within a single acquisition, to quantify MBF and MPR.

The AQUA-MBF (Assessment of Quantitative MBF Using CMR) is a retrospective, observational, international multicenter study involving 10 centers and independent core laboratory readers with the goal of comparing the diagnostic performance of MBF, MPR, and QA for the detection of obCAD. We hypothesized that quantitative stress myocardial blood flow (sMBF) and MPR analysis would identify patients with obCAD as well as experienced physicians in the interpretation of stress CMR.

METHODS

STUDY POPULATION. The study was approved by the Institutional Review Board at each participating site. Participants were enrolled between August 2020 and December 2022 at 10 medical centers across North America, Europe, and Asia. Adults (age >18 years) with known or suspected CAD referred for stress CMR in whom the dual-sequence technique was used, who underwent either an invasive coronary angiography (ICA) or coronary computed tomographic angiography (CTA) within 6 months of stress CMR, were included. Additionally, 18 individuals at very low risk for obCAD were recruited to undergo research stress CMR to capture the full breadth of individuals who might be referred for stress CMR examinations. Patients with myocardial infarction or unstable angina within 30 days, hemodynamically significant ventricular arrhythmia within 30 days, evidence of hemodynamic instability, contraindications to gadolinium-based

From the ᵃDivision of Cardiovascular Medicine, University of Virginia Health System, Charlottesville, Virginia, USA; ᵇDivision of Medicine, University of California, San Diego, San Diego, California, USA; ᶜGE HealthCare, Waukesha, Wisconsin, USA; ᵈDepartment of Diagnostic Radiology, School of Clinical Medicine, Li Ka Shing Faculty of Medicine, University of Hong Kong, Hong Kong, China; ᵉDivision of Cardiovascular Medicine and Department of Radiology, University of Utah School of Medicine, Salt Lake City, Utah, USA; ᶠDepartment of Cardiology, Central DuPage Hospital, Winfield, Illinois, USA; ᵍDepartment of Perioperative Cardiology and Cardiovascular Imaging, Centro Cardiologico Monzino IRCCS, Milan, Italy; ʰDepartment of Medicine and Diagnostic Radiology, McGill University Health Centre, Montreal, Quebec, Canada; ⁱUniversity of Alberta, Edmonton, Alberta, Canada; ʲDepartment of Public Health Sciences, University of Virginia, Charlottesville, Virginia, USA; ᵏDepartment of Nuclear Medicine and PET Center, Aarhus University Hospital, Aarhus, Denmark; ˡDepartment of Cardiology, Stanford University, Stanford, California, USA; ᵐDepartment of Biomedical, Surgical and Dental Sciences, University of Milan, Milan, Italy; ⁿDepartment of Cardiology, Hospital Universitario Quironsalud, Madrid, Spain; ᵒVirginia Heart, Falls Church, Virginia, USA; ᵖInova Schar Heart and Vascular, Fairfax, Virginia, USA; �qDepartment of Medicine, University of Chicago, Chicago, Illinois, USA; ʳHong Kong Sanatorium and Hospital, Hong Kong, China; ˢDepartment of Cardiology, Aarhus University Hospital, Aarhus, Denmark; ᵗDepartment of Diagnostic Radiology, Stanford University, Stanford, California, USA; ᵘDepartment of Cardiology, Ascires Biomedical Group, Valencia, Spain; ᵛDepartment of Nuclear Medicine, University Hospital Zurich, Zurich, Switzerland; ʷCircle Cardiovascular Imaging, Calgary, Alberta, Canada; ˣArea19 Medical, Montreal, Quebec, Canada; ʸGE HealthCare, Munich, Germany; and the ᶻResearch Institute, McGill University Health Centre, Montreal, Quebec, Canada.
Eike Nagel, MD, served as the Guest Editor for this paper.

FIGURE 1 Stress CMR Protocol
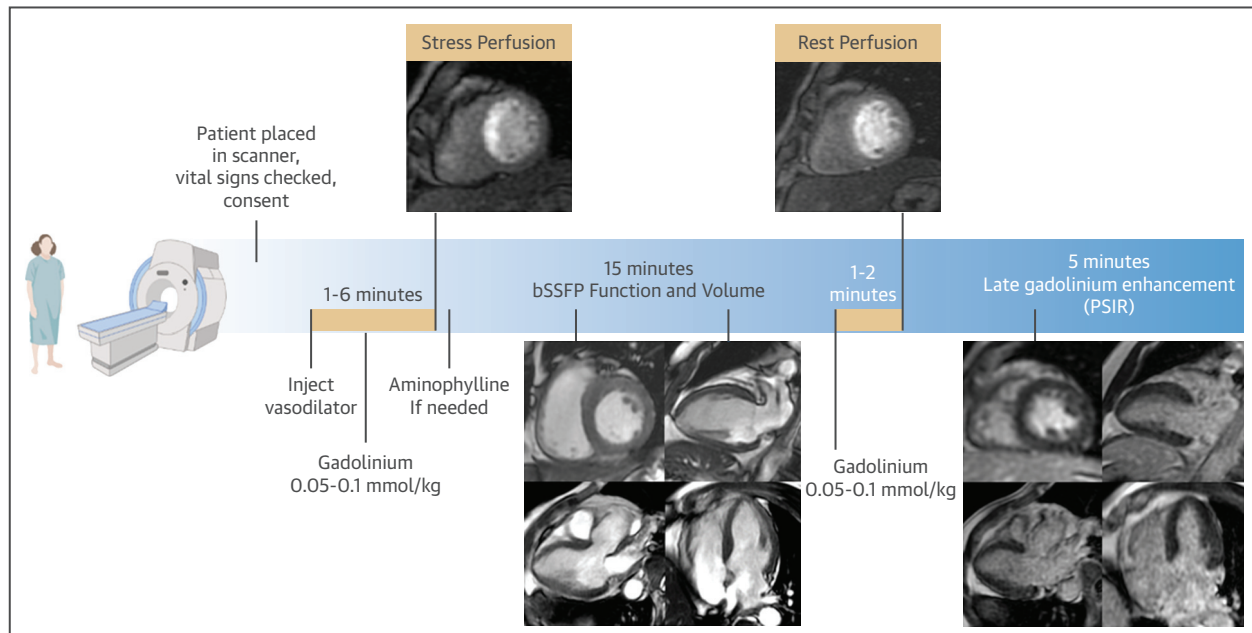
First-pass stress perfusion images are obtained following the administration of regadenoson or adenosine during the infusion of a gadolinium-based contrast agent (GBCA), followed by aminophylline if needed. Next, all functional images are acquired. Resting perfusion images are acquired approximately 15 minutes later during infusion of the GBCA. After an additional 5 minutes, LGE images are acquired. bSSFP = balanced steady-state free precession; CMR = cardiac magnetic resonance; LGE = late gadolinium enhancement; PSIR = phase-sensitive inversion recovery.

contrast agents, advanced renal disease (glomerular filtration rate <30 mL/min/1.73 m^2), severe claustrophobia, current pregnancy, significant bronchospasm, or atrial fibrillation at the time of study enrollment were excluded.

Demographics and comorbidities were collected directly from subjects or extracted from the electronic medical record.

DEFINITION OF obCAD. Each invasive coronary angiographic and coronary computed tomographic angiographic image was interpreted by 2 experienced cardiologists without the availability of CMR findings. If there was a discrepancy, the 2 cardiologists conferred to come to a final determination. The presence of obCAD was defined as stenosis ≥50% in the left main coronary artery or ≥70% in a major vessel on the basis of ICA or coronary CTA. Any individuals with myocardial late gadolinium enhancement (LGE) in an infarct pattern were additionally defined as having obCAD. No obstructive coronary artery disease (noCAD) was defined as absence of myocardial infarction on the basis of LGE and: 1) stenosis <50% in left main coronary artery and <70% in a major coronary artery by ICA or coronary CTA; or

2) an individual at very low risk for obCAD (young age with no cardiac risk factors). Results were also categorized at the per coronary artery level, whereby each coronary artery was categorized according to <50% stenosis, 50% to 69% stenosis, or ≥70% stenosis. Segment-level analysis is reported in the Supplemental Methods.

CMR IMAGE ACQUISITION. Stress CMR imaging (Figure 1) was performed using 1.5-T (SIGNA Artist, GE HealthCare) or 3.0-T (SIGNA Premier, MR750, MR750w, and SIGNA PET/MR, GE HealthCare) scanners. Patients were instructed to abstain from caffeine consumption for 24 hours prior to vasodilator-induced stress CMR. Most centers used a 30-channel anterior array and a 40-channel posterior array coil. Electrocardiographic gating or pulse gating was used, depending on local preferences. For stress imaging, the patient was administered a vasodilator agent, either regadenoson 0.4 mg (injected over approximately 10 seconds into a peripheral vein) or adenosine (140 μg/kg/min with up-titration if needed for 3-5 minutes, followed by a 5-mL saline flush). Dual-sequence perfusion was acquired for approximately 70 heartbeats following vasodilator

FIGURE 2   Perfusion Image Acquisition and Quantitative Perfusion Technique
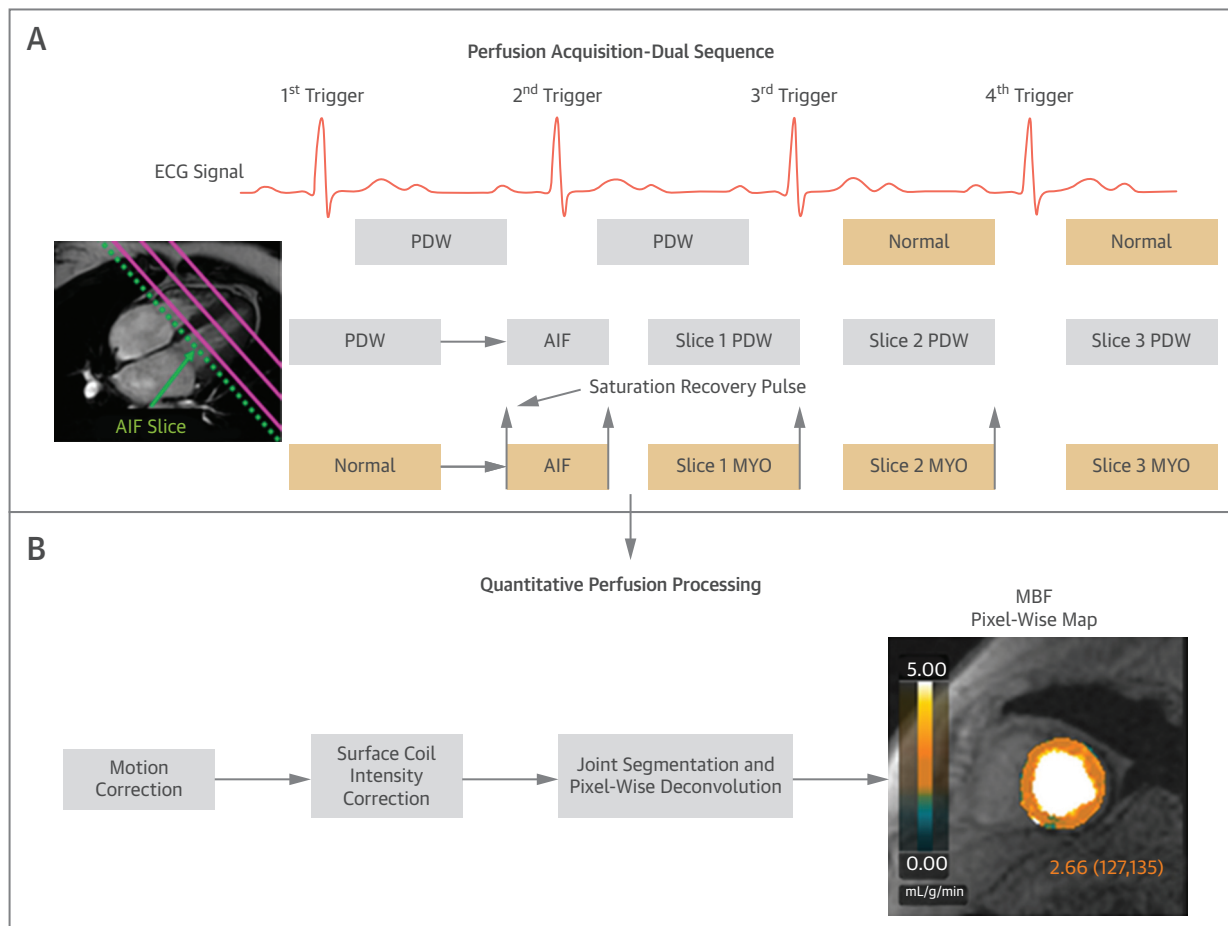
(A) Dual saturation–prepared sequence and typical slice positions. (B) Postprocessing steps for quantitative perfusion. AIF = arterial input function; ECG = electrocardiographic; MBF = myocardial blood flow; MYO = myocardium; PDW = proton density weighted.

administration and during the first pass of the gadolinium-based contrast agent (0.05-0.1 mmol/kg, injected at a rate of 2-4 mL/s). Aminophylline 50-100 mg or caffeine citrate 60 mg was administered intravenously for reversal of hyperemia after stress imaging in cases of regadenoson. At 5 to 15 minutes after stress imaging, rest perfusion was performed during the infusion of a gadolinium-based contrast agent (0.05-0.1 mmol/kg), followed by a saline flush (50 mL). Cine and LGE images were acquired in accordance with Society for Cardiovascular Magnetic Resonance guidelines.

CMR PERFUSION IMAGING. For perfusion imaging (**Figure 2A**), a free-breathing, dual-sequence technique used saturation preparation with spoiled gradient echo time to acquire the AIF image, along with 3 myocardial short-axis slices of the left ventricle, during both stress and rest conditions. The AIF image has low spatial but high temporal resolution (about one-third acquisition duration compared with normal myocardial slices); other parameters of AIF imaging include slice thickness of 8 mm, a flip angle of 5°, and a saturation recovery time of about 10 ms. Myocardial short-axis slice perfusion imaging parameters were as follows: slice thickness of 8 mm, a variable interslice gap (8-24 mm) to accommodate adequate spacing of slices through the left ventricle, repetition time of 2.7 to 4.0 ms, echo time of 1.0 to 1.7 ms, a flip angle of 15°, partial Fourier 0.75, a parallel imaging factor of 2, a field of view of 36-50 × 27-38 cm, and an acquired matrix of 192 × 148 pixels. Proton-density-weighted images were also acquired for the first 2 frames of each slice to correct the inhomogeneity of surface coil–related signal intensity.

FIGURE 3 Example of noCAD
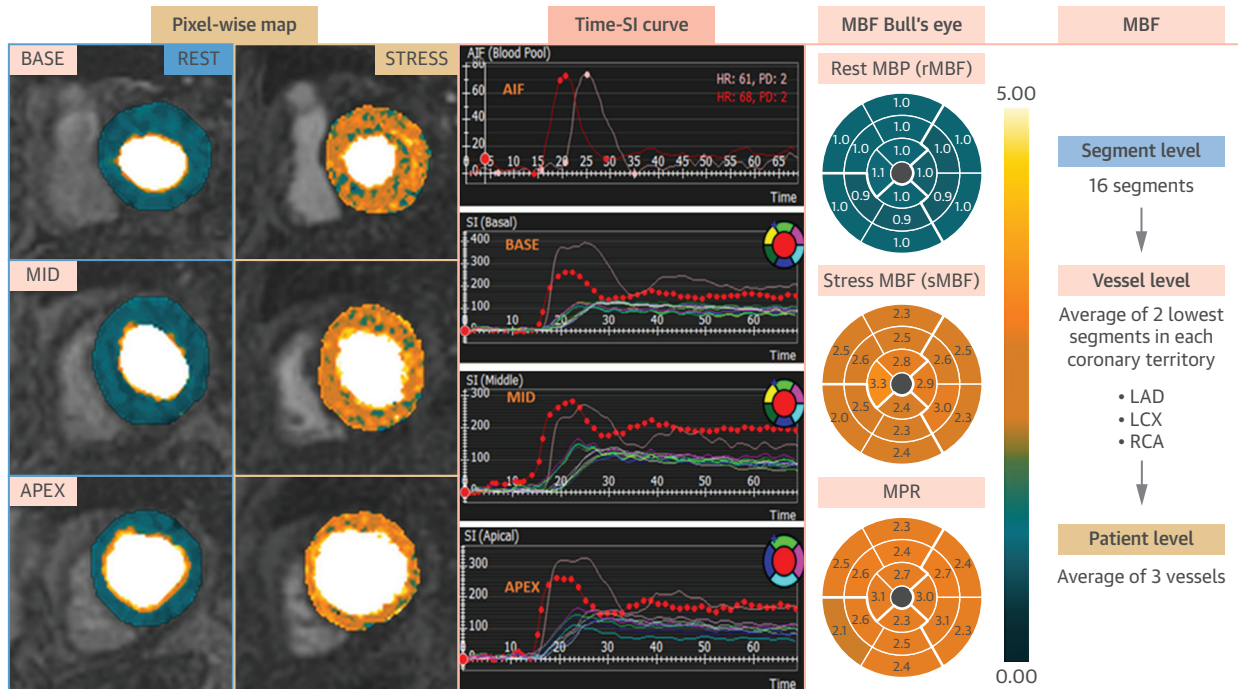
(A) Pixelwise MBF mapping at rest and during stress. (B) Signal intensity curves for AIF, basal, mid, and apical myocardium. (C) Rest myocardial blood flow (rMBF), stress myocardial blood flow (sMBF), and myocardial perfusion reserve (MPR) for each of the 16 American Heart Association segments shown as a bull's-eye plot. (D) Method of MBF calculation for the segment-level, vessel level, and patient level. LAD = left anterior descending coronary artery; LCX = left circumflex coronary artery; noCAD = no obstructive coronary artery disease; RCA = right coronary artery; SI = signal intensity; other abbreviations as in **Figure 2**.

CMR IMAGE ANALYSIS. All analysis was performed in a blinded fashion by the core laboratory. Images were analyzed using commercially available software (cvi42, Circle Cardiovascular Imaging). Left ventricular (LV) and right ventricular end-diastolic and end-systolic frames were identified from short-axis cine images, with the Simpson disk summation method applied to calculate LV mass and LV and right ventricular end-diastolic and end-systolic volumes, with the corresponding ejection fractions. LGE was categorized by visual inspection as an infarct pattern being present or absent.

PERFUSION IMAGE ANALYSIS. Qualitative and quantitative analysis of the perfusion images was performed by different members of the core laboratory. Blinded QA was performed independently by 4 cardiologists with stress CMR experience ranging from 5 to 20 years. Each evaluated all cases and was blinded to all clinical data and findings on ICA or coronary CTA. QA used a 5-point scale (1 = definitely abnormal, 2 = probably abnormal, 3 = indeterminate,

4 = probably normal, and 5 = definitely normal), with scoring conducted on a per patient and per coronary artery territory basis. Each core laboratory reader was provided the following diagnostic criteria to standardize the definition of a perfusion defect: 1) a perfusion defect occurs after contrast arrives in the LV myocardium; 2) a perfusion defect persists beyond peak myocardial enhancement for at least 4 R-RR intervals; 3) a perfusion defect is more than 1 pixel wide; and 4) dark-rim artifact is considered to be unlikely.

For QP analysis, first-pass images were analyzed (**Figure 2B**) using cvi42 version 2774. One QP reader, who had trained on 350 cases, performed MBF analysis. The QP analysis results, independently conducted by the second QP reader with identical training, were used for the interobserver test. The average time for QP analysis for each case was approximately 15 minutes. The first 70 frames of the perfusion sequence were used for analysis. Motion correction was applied to compensate for respiratory and cardiac motion.[11] Surface-coil intensity correction

TABLE 1 Patient Demographics and Clinical Characteristics			
	Overall (N = 127)	noCAD (n = 71)	obCAD (n = 56)	P Value
Age, y	65 (57-74)	60 (42-67)	71 (64-77)	<0.001
Obesity	23 (18)	9 (13)	14 (25)	0.119
Male	84 (67)	38 (54)	46 (84)	<0.001
Ethnicity	84 (67)	38 (54)	46 (84)	0.001
White	88 (70)	39 (55)	49 (89)	0.001
Black	4 (3)	1 (1)	3 (6)	0.320
Asian	22 (17)	21 (30)	1 (2)	0.001
Mixed	4 (3)	4 (6)	0 (0)	0.094
Unknown	8 (6)	6 (8)	2 (4)	0.464
Medical history			
Prior MI	30 (24)	4 (6)	26 (47)	<0.001
Prior PCI or CABG	64 (48)	16 (23)	48 (87)	<0.001
Heart failure	9 (7)	2 (3)	7 (13)	0.041
Comorbidities			
Smoker	28 (22)	10 (14)	18 (33)	0.013
Diabetes	46 (37)	28 (39)	18 (33)	0.438
Hypertension	85 (67)	42 (59)	43 (78)	0.024
Hyperlipidemia	83 (66)	38 (54)	45 (82)	<0.001
Chronic renal disease	7 (6)	4 (6)	3 (6)	1
Post–heart transplantation	4 (3)	4 (6)	0 (0)	0.131

Values are median (Q1-Q3) or n (%), unless otherwise indicated

CABG = coronary artery bypass graft surgery; MI = myocardial infarction; noCAD = no obstructive coronary artery disease; obCAD = obstructive coronary artery disease; PCI = percutaneous coronary intervention.

was processed automatically to correct B1 field-related inhomogeneity in the perfusion images.[12] The LV endocardial and epicardial boundaries were automatically generated by the software on the perfusion and AIF images at rest and stress, with manual adjustments when needed. Once ventricular segmentation and heart rate were verified, pixelwise resting and sMBF maps (Figure 3A) were displayed along with corresponding segmental time–signal intensity curves (Figure 3B) according to the 16-segment model. MBF values were reported in milliliters per minute per gram and derived using deconvolution of the AIF and tissue perfusion time-intensity curves, with the resulting impulse response being constrained to a Fermi function. A logistic impulse response function was applied to the traditional Fermi function, as previously described.[13] Segmental MBF values were automatically derived using the median MBF pixel values to produce bull's-eye plots displaying segmental rest MBF (rMBF), sMBF, and MPR (the ratio between sMBF and rMBF) (Figure 3C). Segments were excluded from the analysis if they exhibited the following characteristics: 1) thin myocardium significantly affected by partial volume effects from the LV cavity signal; 2) segments affected by excessive motion artifact; and 3) segments that included the LV outflow tract. The remaining

segments were used to calculate rMBF, sMBF, and MPR values on a per patient level, coronary artery level, and segment level. For the coronary artery territory level, the MBF was calculated as the average of 2 segments with the lowest values in the corresponding coronary artery territory. For the patient level, 2 methods were tested. The first method was the global MBF calculated as the average of 3 coronary artery territory MBF values and referred to as global mean MBF. The other method is referred to as global minimum MBF, which is defined as the lowest MBF value of the 3 coronary artery territories (Figure 3D).

The occurrence of 2 R-R interval acquisitions and significant residual cardiac motion were recorded. Two R-R interval acquisition refers to the acquisition of 3 slices every 2 R-R intervals, rather than every R-R interval. Cardiac motion is defined as when the perfusion images had at least 1 slice series in which several images were acquired during different phases of the cardiac cycle caused by improper gating.

STATISTICAL ANALYSIS. The normality of distribution of continuous variables was tested using the 1-sample Kolmogorov-Smirnov test. Continuous variables with normal distributions are expressed as mean ± SD and were compared between the obCAD and noCAD groups using Student's t-test; skewed variables are reported as median (Q1-Q3) and were compared between groups using the Wilcoxon rank-sum test. Categorical variables are presented as absolute numbers with percentages and were compared between groups using the chi-square test or Fisher exact test if at least 1 cell count was <5. Logistic regression with the interaction term was used to test whether patient characteristics or technical acquisition factors would affect the relationship between obCAD and stress CMR measurements. The restricted cubic spline function was performed to test the nonlinear relationship between CMR measurements and the probability of obCAD. The spline function is constructed by dividing the x-axis into 5 segments and fitting a polynomial function to each segment. Receiver-operating characteristic (ROC) curve analysis and the corresponding area under the curve (AUC) was used to quantify the overall diagnostic accuracy of identifying obCAD. The Youden index was used to determine the optimal threshold of MBF and MPR cutoff values. Comparison of ROC curves was performed using DeLong test. A nonparametric meta-analysis random-effects model was used to estimate a combined ROC curve by weighting each individual interpolated ROC curve on the basis of the QA of the 4 cardiologists, taking into account the variability between the raters. A linear mixed-effects

model with per patient random effect was used to account for the clustering of multiple vessel measurements. The inter-rater reliability between the 2 cardiologists' readings of ICA and coronary CTA was measured using Cohen's kappa coefficient. The inter-rater reliability among the 4 cardiologists for QA was measured using Fleiss's kappa coefficient. The inter-class correlation coefficient for interobserver variability for QP analysis by 2 readers was calculated for all 127 subjects, and intraobserver variability was assessed by randomly selecting 20 subjects, using a 2-way random-effects model. Values of $P < 0.05$ were considered to indicate statistical significance. Analyses were performed using R version 4.2.3 (R Foundation for Statistical Computing), SPSS Statistics for Windows version 25.0 (IBM), and Prism version 9.4.1 (GraphPad Software).

RESULTS

BASELINE CHARACTERISTICS AND CAD STATUS.
Patient characteristics are shown in Table 1. One hundred fifty subjects were included in the study, but 23 subjects were excluded because of a duration of >6 months between stress CMR and ICA or coronary CTA. Thus, 127 individuals were included for analysis (Supplemental Figure 1). Seventy-seven patients underwent ICA, 32 underwent coronary CTA, and 18 had a very low pretest probability for CAD. The median duration between stress CMR and ICA or coronary CTA was 24 days (Q1-Q3: 7-49 days). Patient demographics are shown in Table 1.

Fifty-six patients (44%) had obCAD, while 71 subjects (56%) had noCAD. noCAD was defined using coronary CTA in 31 subjects and ICA in 22 patients. obCAD was defined using coronary CTA in 1 participant and ICA in 55 subjects. Eight patients with obCAD had stenoses ≤70% in all 3 coronary territories but had infarct-related LGE. Twenty-two subjects (39%) had single-vessel disease, 21 (38%) had double-vessel disease, and 13 (23%) had 3-vessel disease. CMR measurements are shown in Table 2.

ACQUISITION DETAILS DURING STRESS CMR.
Eighty-two CMR examinations (65%) were performed on a 1.5-T scanner and 45 (35%) on a 3.0-T scanner. Eighty-nine subjects (70%) underwent stress perfusion before rest, and 38 (30%) underwent rest perfusion first. Adenosine was used in 36 subjects (28%) and regadenoson in 91 (72%) subjects. First-pass perfusion imaging was performed using a high-relaxivity contrast agent in 106 subjects (83.5%) and a low-relaxivity contrast agent in 21 (16.5%).

COMPARISON OF MBF AND MPR BETWEEN obCAD AND noCAD.
At the patient level (Table 3), global

TABLE 2 Stress CMR Imaging Measurements				
	Overall (N = 127)	noCAD (n = 71)	obCAD (n = 56)	P Value
Hemodynamic parameters				
Rest heart rate, beats/min	66 (59-77)	66 (57-77)	66 (60-76)	0.621
Stress heart rate, beats/min	90 ± 18	96 ± 18	82 ± 15	<0.001
CMR parameters				
LVEF, %	59 (54-63)	60 (55-63)	58 (48-61)	0.002
LVEDVI, mL/m^2	74 (65-86)	77 (67-90)	72 (64-85)	0.316
LVESVI, mL/m^2	31 (25-41)	31 (25-39)	31 (24-42)	0.817
LVMI, g/m^2	52 (46-60)	50 (45-57)	56 (50-66)	0.001
RVEF, %	57 (54-61)	57 (53-61)	58 (55-61)	0.406
RVEDVI, mL/m^2	73 ± 17	78 ± 18	67 ± 14	0.001
RVESVI, mL/m^2	32 (23-39)	34 ± 10	29 ± 11	0.011
LGE	39 (31)	5 (7)	34 (61)	<0.001
Infarct pattern	33 (26)	0 (0)	33 (59)	<0.001
Noninfarct pattern	7 (5)	5 (7)	2 (4)	

Values are median (Q1-Q3), mean ± SD, or n (%), unless otherwise indicated.

CMR = cardiac magnetic resonance; LGE = late gadolinium enhancement; LVEDVI = left ventricular end-diastolic volume index; LVEF = left ventricular ejection fraction; LVESVI = left ventricular end-systolic volume index; LVMI = left ventricular mass index; RV = right ventricular; RVEDVI = right ventricular end-diastolic volume index; RVEF = right ventricular ejection fraction; RVESVI = right ventricular end-systolic volume index; other abbreviations as in Table 1.

mean sMBF was significantly lower in the obCAD group than in the noCAD group. Global mean MPR was significantly lower in the obCAD group than in the noCAD group. The comparison of global minimum rMBF, minimum sMBF, and minimum MPR between the 2 groups was similar to global mean rMBF, mean sMBF, and mean MPR (Table 3). The association between CAD groups and either global mean sMBF (Figure 4A) or global mean MPR (Figure 4C) was not affected by age, sex, hypertension, hyperlipidemia, diabetes mellitus, or smoking status. Additionally, there was no apparent impact between the association between CAD groups and global mean sMBF by technical examination factors. However, excessive cardiac motion may influence the association between global mean sMBF and obCAD ($P = 0.007$) (Figure 4B). Additionally, the association between global mean MPR and obCAD may be affected by whether stress imaging or rest imaging was performed first (Figure 4D). The association between CAD groups and global minimum sMBF or minimum MPR was similar to global mean sMBF or mean MPR (Supplemental Figure 2).

Segment-level analysis is reported in the Supplemental Methods, Supplemental Table 1, Supplemental Figures 3 and 4.

At the coronary territory level, MPR and sMBF were significantly lower in vessels with obCAD compared with those with noCAD (Table 3). There were no significant differences in the diagnostic performance for the detection of a coronary artery with ≥50% stenosis and ≥70% stenosis in both sMBF and MPR (Table 3).

TABLE 3 Comparison of rMBF, sMBF, and MPR Between noCAD and obCAD at the Patient Level and Vessel Level

	noCAD (n = 71)	obCAD (n = 56)	P Value		noCAD (n = 71)	obCAD (n = 56)	P Value
Patient level							
Global mean rMBF, mL/g/min	1.00 (0.86-1.15)	1.05 (0.91-1.18)	0.30	Global minimum rMBF, mL/g/min	0.95 (0.75-1.03)	0.95 (0.85-1.04)	0.51
Global mean sMBF, mL/g/min	2.38 (2.13-2.74)	1.53 (1.21-1.78)	<0.001	Global minimum sMBF, mL/g/min	2.15 (1.90-2.52)	1.30 (0.99-1.50)	<0.001
Global mean MPR	2.05 (1.64-2.71)	1.31 (1.01-1.55)	<0.001	Global minimum MPR	1.79 (1.45-2.45)	1.11 (0.90-1.36)	<0.001

	noCAD (n = 278)			obCAD (n = 103)			
Vessel level							
rMBF, mL/g/min	1.00 (0.90-1.14)			1.01 (0.90-1.17)			0.19
sMBF, mL/g/min	2.25 (1.85-2.65)			1.45 (1.12-1.78)			<0.001
MPR	1.90 (1.43-2.41)			1.20 (0.93-1.53)			<0.001

	Stenosis <50% (n = 258)	Stenosis 50%-69% (n = 20)	Stenosis ≥70% (n = 103)	P Value
rMBF, mL/g/min	1.00 (0.90-1.14)	1.02 (0.91-1.11)	1.01 (0.90,1.17)	0.71
sMBF, mL/g/min	2.28 (1.90-2.68)[a,b]	1.51 (1.30-2.14)	1.45 (1.12-1.78)	<0.001
MPR	1.94 (1.47-2.56)[a,b]	1.39 (1.11-1.75)	1.20 (0.93-1.53)	<0.001

Values are median (Q1-Q3), unless otherwise indicated. [a]$P < 0.05$ vs stenosis 50% to 69%. [b]$P < 0.05$ vs stenosis ≥70%.

MPR = myocardial perfusion reserve; rMBF = rest myocardial blood flow; sMBF = stress myocardial blood flow; other abbreviations as in Table 1.

DIAGNOSTIC PERFORMANCE OF QP. At the patient level, ROC analysis showed that global mean sMBF and mean MPR had AUCs of 0.90 (95% CI: 0.84-0.96) and 0.86 (95% CI: 0.80-0.93), respectively, for detecting obCAD (Figure 5A). A cutoff value of 2.04 mL/g/min for global mean sMBF achieved the best specificity, sensitivity, and accuracy (Table 4). With this cutoff, there were 6 false-negative patients without LGE on the basis of global mean sMBF. Two of them had single-vessel stenosis >70%, Four of them had histories of percutaneous coronary intervention. In all 4 patients, the stenosis was in another vessel and not in-stent restenosis. The optimal cutoff value of 1.61 for global mean MPR had good sensitivity but low specificity because of high global mean rMBF. There was no significant difference in ROC between global mean sMBF and global mean MPR at the patient level (0.897 vs 0.864; $P = 0.247$). Global minimum sMBF and minimum MPR had similar AUCs to global mean sMBF and mean MPR. A cutoff value of 1.85 mL/g/min for global minimum sMBF and 1.44 for global minimum MPR corresponded to the best specificity, sensitivity, and accuracy (Table 3).

For the coronary artery territory, ROC analysis showed that sMBF and MPR had excellent AUCs of 0.82 (95% CI: 0.78-0.87) and 0.81 (95% CI: 0.77-0.86), respectively, to detect obCAD (Figure 5B, Table 5). There was no significant difference in AUCs between sMBF and MPR at the coronary artery level ($P = 0.55$). A cutoff value of 1.95 mL/g/min for sMBF and 1.58 for MPR achieved the best specificity, sensitivity, and accuracy.

COMPARISON OF QA AND QP. QA of stress CMR imaging was performed by 4 experts at both the patient level and coronary territory level (Table 4, Supplemental Figure 5). At the patient level, the AUCs for the 4 readers ranged between 0.69 and 0.89. Compared with the AUC of global mean sMBF, 2 readers had similar AUCs ($P = 0.617$ and $P = 0.445$), while the other had significantly lower AUCs ($P < 0.01$ for both). The mean AUC of the 4 readers was 0.796 (95% CI: 0.733-0.858), with an upper 95% confidence limit less than the AUC of mean sMBF (0.897) and minimum sMBF (0.895) (Figure 5A, Table 4). The mean AUC of the 4 readers had an upper 95% confidence limit less than the AUC of mean MPR (0.864) but greater than the AUC of minimum MPR 0.852 (Figure 5A, Table 4). At the coronary artery territory level, the AUCs for the 4 readers ranged between 0.64 and 0.80. The AUCs for sMBF and MPR were similar to 2 of the readers ($P = 0.162$ and $P = 0.320$) but better than the other 2 readers ($P < 0.01$ for both) at the coronary territory level. The mean AUC of the 4 readers was 0.725 (95% CI: 0.683-0.768), with an upper 95% confidence limit less than the AUC of sMBF (0.823) (Figure 5B, Table 5). The mean AUC of the 4 readers had an upper 95% CI less than the AUC of MPR (0.812) (Figure 5B, Table 5). Thus, the average AUC for the 4 readers was significantly lower than sMBF and MPR on the basis of the 95% CI.

REPRODUCIBILITY. The inter-rater reliability between the 2 cardiologists' readings of the invasive coronary angiographic and coronary computed

FIGURE 4 Effect Modification of the Association Between Global Mean MBF and obCAD at the Patient Level
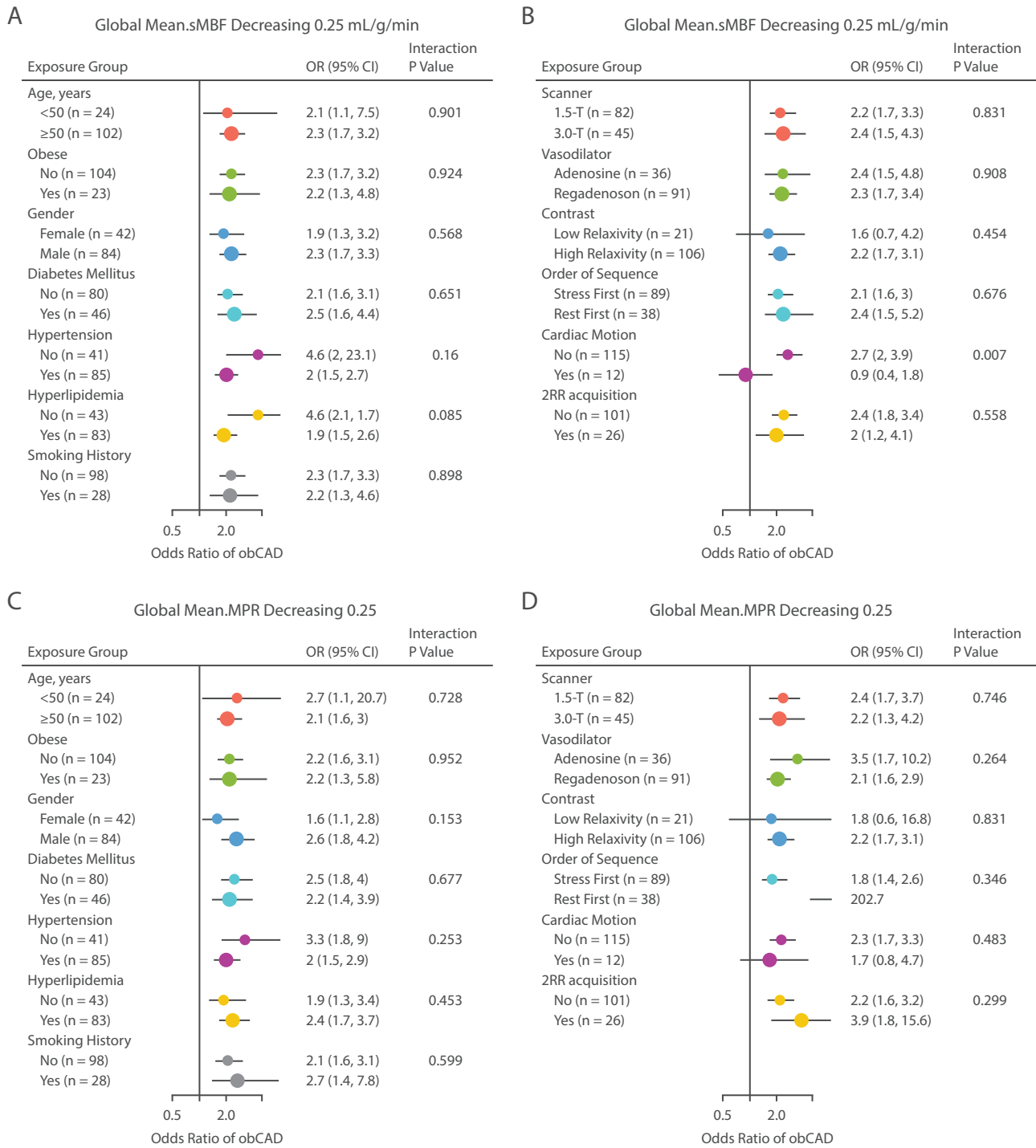
(A) Global mean sMBF and obstructive coronary artery disease (obCAD) for different clinical variables. (B) Global mean sMBF and obCAD for different technical variables. (C) Global mean MPR and obCAD for different clinical variables. (D) Global mean MPR and obCAD for different technical variables. 2RR = 2 R-R intervals; other abbreviations as in **Figures 2 and 3**.

FIGURE 5 Diagnostic Performance of QP and QA

Receiver-operating characteristic (ROC) curve for mean sMBF, global mean MPR, and qualitative assessment (QA) for the detection of obCAD at the patient level (A) and at the coronary artery level (B). Curves A, B, C, and D in gray represent 4 experienced readers. The blue curve is the average ROC of the readers. AUC = area under the curve; QP = quantitative perfusion; other abbreviations as in Figures 3 and 4.

tomographic angiographic images had a Cohen's kappa coefficient of 0.93 (95% CI: 0.90-0.97) for the coronary vessel level. The inter-rater reliability among the 4 cardiologists for QA had a Fleiss's kappa coefficient of 0.39 (95% CI: 0.32-0.47). The intraclass correlation coefficient for the intraobserver variability of QP was 0.90 (95% CI: 0.86-0.92) for rMBF, 0.93 (95% CI: 0.89-0.95) for sMBF, and 0.86 (95% CI: 0.81-0.90) for MPR. For rMBF, the intraclass correlation coefficient for the interobserver variability of QP was 0.90 (95% CI: 0.88-0.92) for the per vessel level and 0.92 (95% CI: 0.88-0.94) for the per patient level. For sMBF, it was 0.93 (95% CI: 0.91-0.94) and 0.96 (95% CI: 0.94-0.97). For MPR, it was 0.92 (95% CI: 0.90-0.93) and 0.96 (95% CI: 0.94-0.97), respectively (Supplemental Table 2, Supplemental Figure 6).

DISCUSSION

In this international multicenter study, we demonstrate that sMBF and MPR quantification using stress CMR can differentiate obCAD from noCAD at the patient level and the coronary artery territory level. Proposed thresholds of sMBF of <2.04 mL/g/min and MPR of 1.61 provided good diagnostic performance for detecting obCAD at the patient level. Additionally, the probability that obCAD was present decreased

logarithmically as sMBF increased from 2.04 mL/g/min. The association between sMBF and obCAD was independent of the effect of cardiovascular risk factors and most aspects related to acquisition technique. Additionally, global sMBF had superior performance compared with QA performed by some experts for the detection of obCAD (Central Illustration).

QUANTIFICATION OF MBF USING STRESS CMR. With the advent of the dual-sequence, first-pass perfusion technique[14] and the development of robust and user-friendly software analysis tools,[6] absolute quantification of MBF using stress CMR has become clinically feasible. In this study, we expand our understanding of MBF analysis using stress CMR to a second CMR vendor and in a multicenter setting.

The global rMBF, sMBF, and MPR values seen in individuals with obCAD were comparable with those reported by other studies. Biglands et al[10] reported rMBF of 1.23 ± 0.41 mL/g/min, sMBF of 2.16 ± 0.70 mL/g/min, and MPR of 1.86 ± 0.57 in individuals with obCAD. Their cohort had a similar proportion of patients with prior myocardial infarction and LGE included as our study but had lower rMBF, sMBF, and MPR than in our study. sMBF values for the noCAD cohort of patients in our study were lower than

TABLE 4 Diagnostic Performance of Global Mean sMBF, Global Mean MPR, Global Minimum sMBF, and Global Minimum MPR and Visual Assessment (QA) for Obstructive Coronary Artery Disease at the Patient Level

	AUC (95% CI)	Specificity (95% CI)	Sensitivity (95% CI)	Accuracy	PPV	NPV	Threshold
Global mean sMBF	0.897 (0.84-0.96)	0.86 (0.76-0.92)	0.89 (0.74-0.92)	0.87	0.86	0.86	2.04 mL/g/min
Global minimum sMBF	0.896 (0.84-0.95)	0.85 (0.74-0.91)	0.88 (0.76-0.94)	0.86	0.82	0.90	1.85 mL/g/min
Global mean MPR	0.864 (0.80-0.93)	0.79 (0.66-0.86)	0.82 (0.66-0.89)	0.80	0.75	0.85	1.61
Global minimum MPR	0.852 (0.79-0.92)	0.76 (0.65-0.84)	0.82 (0.70-0.90)	0.79	0.73	0.84	1.44
QA_A	0.89 (0.83-0.95)	0.80 (0.78-0.93)	0.89 (0.64-0.86)	0.84	0.78	0.90	
QA_B	0.87 (0.83-0.94)	0.87 (0.70-0.88)	0.74 (0.80-0.96)	0.82	0.82	0.82	
QA_C	0.74 (0.66-0.83)[a,b,c,d]	0.82 (0.72-0.89)	0.55 (0.43-0.69)	0.70	0.70	0.70	
QA_D	0.69 (0.59-0.78)[a,b,c,d]	0.94 (0.87-0.98)	0.45 (0.33-0.58)	0.72	0.86	0.68	

[a]P < 0.01 vs global mean sMBF. [b]P < 0.01 vs global mean MPR. [c]P < 0.01 vs global minimum sMBF. [d]P < 0.01 vs global minimum MPR.

AUC = area under curve; NPV = negative predict value; PPV = positive predict value; QA = qualitative assessment; other abbreviations as in Table 3.

previous reports derived from healthy volunteers; this is likely because patients with noCAD still have multiple comorbidities that are known to affect MBF through alterations in coronary microvascular function.

It would be anticipated that myocardial segments supplied by a noCAD vessel would exhibit higher sMBF than segments supplied by an obCAD vessel. In a study by Hsu et al,[6] sMBF was 0.9 ± 0.4 in ischemic segments and 2.3 ± 0.6 mL/g/min in remote segments.[6] We did not observe such a magnitude of difference in the segmental sMBF values for vessels with obCAD vs those with noCAD. One theoretical explanation for this is that our cohort may have had a higher prevalence of coronary microvascular disease that decreased the sMBF values in patients with noCAD.[7] Additionally, we used a different scanner vendor, pulse sequence readout, and the use of a mixture of adenosine and regadenoson as the vasodilator, which might explain the discrepancy of observed sMBF in the ischemic segments between the 2 studies. However, it is reassuring that the diagnostic performance of sMBF in our study was similar to that published by Hsu et al.[6]

In the present study, MBF quantification was performed using the deconvolution technique, with the resulting impulse function being constrained to a Fermi function. This approach for quantifying MBF is in contrast to other studies that relied on the blood tissue exchange model.[7,8] Despite using a different model for quantifying MBF, our global sMBF cutoff value (<2.04 mL/g/min) and coronary artery territory sMBF cutoff value (<1.95 mL/g/min) for detecting obCAD were consistent with that reported using the blood tissue exchange model (<1.94 mL/g/min).[7] The diagnostic performance for detecting obCAD was also similar for both blood flow models. At the moment, there is no consensus about which model for quantifying MBF from stress CMR images should be used; consequently, the blood flow models used by different vendors may vary.

The diagnostic performance of MPR for the detection of obCAD trended lower than sMBF in our study. This may be caused by performing stress perfusion first, which can cause lingering effects upon resting MBF and thereby result in a lower MPR, despite reversal with aminophylline or caffeine. Additionally, the time to resting perfusion after the administration of aminophylline was variable in our study, making it likely that MPR values measured in our study may have had some unintended variability, reducing their diagnostic performance. Currently there are

TABLE 5 Diagnostic Performance of sMBF, MPR, and Visual Assessment (QA) for Obstructive Coronary Artery Disease at the Vessel Level

	AUC (95% CI)	Specificity (95% CI)	Sensitivity (95% CI)	Accuracy	PPV	NPV	Threshold
sMBF	0.823 (0.78-0.87)	0.69 (0.64-0.75)	0.87 (0.80-0.92)	0.74	0.51	0.94	1.95 mL/g/min
MPR	0.812 (0.77-0.86)	0.67 (0.62-0.73)	0.79 (0.70-0.85)	0.70	0.47	0.89	1.58
QA_A	0.80 (0.76-0.86)	0.59 (0.56-0.67)	0.87 (0.79-0.92)	0.66	0.44	0.92	
QA_B	0.76 (0.71-0.82)	0.83 (0.78-0.87)	0.59 (0.49-0.68)	0.76	0.56	0.84	
QA_C	0.68 (0.62-0.73)[a,b]	0.91 (0.87-0.93)	0.38 (0.29-0.47)	0.76	0.60	0.79	
QA_D	0.64 (0.59-0.72)[a,b]	0.94 (0.91-0.97)	0.32 (0.24-0.41)	0.72	0.86	0.68	

[a]P < 0.01 vs sMBF. [b]P < 0.01 vs MPR.

Abbreviations as in Tables 3 and 4.

CENTRAL ILLUSTRATION Diagnostic Performance of Quantitative Myocardial Blood Flow Analysis for the Detection of Obstructive Coronary Artery Disease
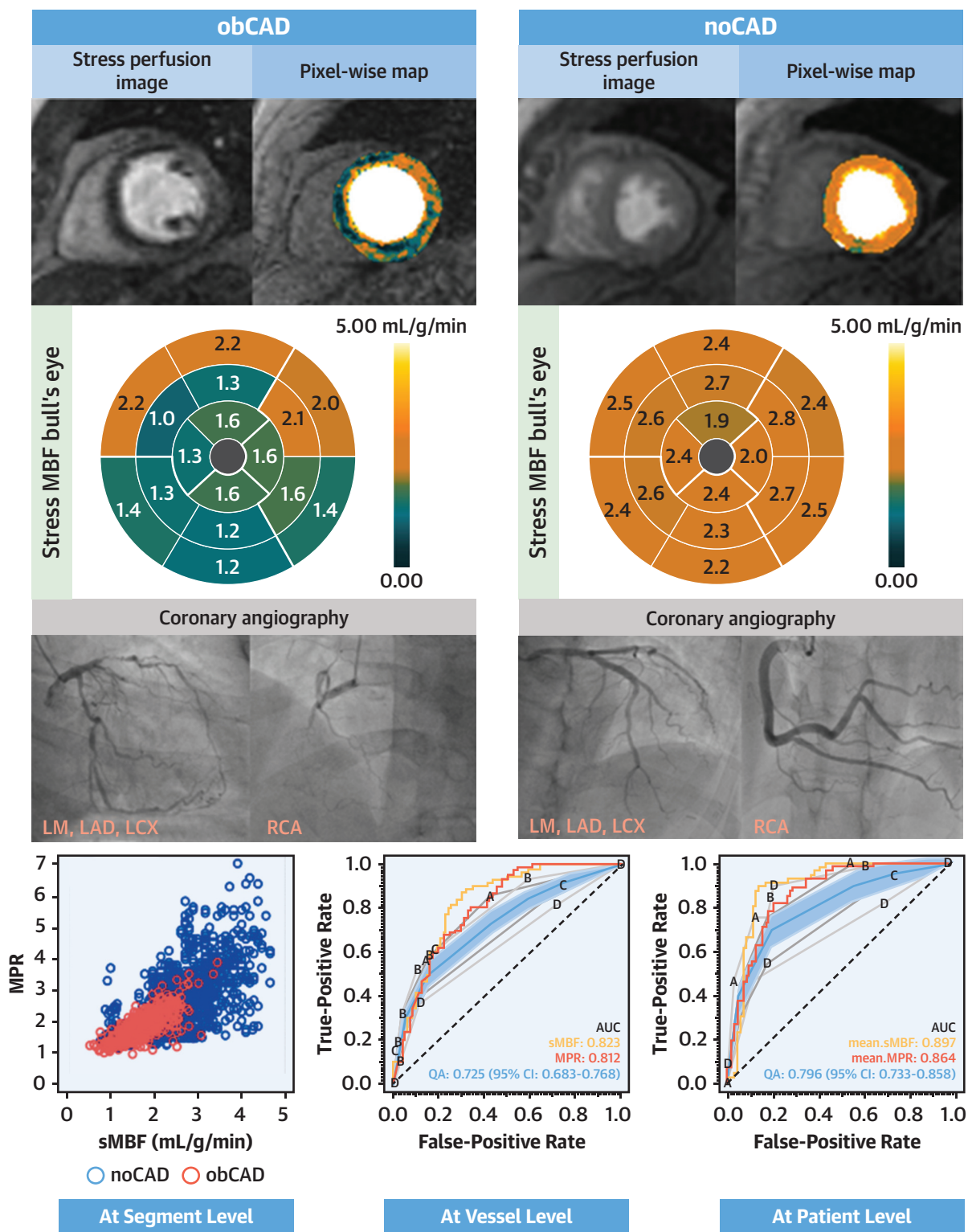
Wang S, et al. JACC Cardiovasc Imaging. 2024;■(■):■-■.

AUC = area under the curve; LM = left main coronary artery; LAD = left anterior descending coronary artery; LCX = left circumflex coronary artery; MPR = myocardial perfusion reserve; noCAD = no obstructive coronary artery disease; obCAD = obstructive coronary artery disease; RCA = right coronary artery; sMBF = stress myocardial blood flow.

insufficient data to determine the optimal time following the administration of aminophylline to derive an accurate and reproducible MPR value. This variability in MPR measurement can be obviated by performing resting perfusion first to acquire a true resting blood flow value, followed by stress perfusion imaging to derive the sMBF value; however, it is unclear if a rest-first strategy of stress CMR may reduce the ability to qualitatively assess the stress CMR examination.

DIAGNOSTIC PERFORMANCE OF QUALITATIVE VS QUANTITATIVE STRESS CMR. Stress CMR is an accurate test for the detection of obCAD; however, the technique is not widely available, and interpretation requires considerable expertise. In our study, the average AUC of visual interpretation performed by experts was excellent (0.80); however, there was considerable variability among the readers. It is likely that the variability in image interpretation will increase as a larger number of individuals begin to interpret stress CMR. Quantification of MBF has the potential to diminish inter-reader variability, while also providing quantitative data that can be incorporated into the interpretation of the study. We also performed a sensitivity analysis of the quantitative stress CMR technique in multiple scenarios (different field strengths, contrast agents, vasodilators, rest-first vs stress-first protocols, and in patients with a wide range of pre-existing risk factors). Quantitative sMBF was consistently able to differentiate obCAD from noCAD across most of these scenarios.

STUDY LIMITATIONS. Our study had a retrospective design, and the overall sample size was relatively small. Another limitation is that we did not use invasive FFR as the reference standard; however, as the same reference standard was used to define the accuracy of quantitative MBF analysis and QA, the conclusion of the study that quantification of MBF is more accurate than QA performed by experts is unlikely to change. Additionally, our patient cohort includes patients with both high and low pretest probability, which could lead a reviewer blinded to clinical history to either overcall or undercall abnormalities. The use of coronary CTA could be considered another limitation. The degree of stenosis can be overestimated on coronary CTA in the presence of stenosis; however, in our coronary CTA cohort, only 1 patient had a stenosis of ≥70%. Another challenge encountered in this study is that 8 subjects had histories of myocardial infarction that was previously revascularized. These subjects were classified in the obCAD group despite not having significant stenoses within their stents because their sMBF was reduced as

a consequence of their chronic myocardial scar. A reader blinded to clinical data would have no way of knowing this clinical history. Our study does not allow us to understand the diagnostic performance of MBF analysis in patients with prior myocardial infarction. It is unknown if our findings can be extrapolated to other vendors' scanners and QP algorithms. Our cohort was composed of individuals with predominantly preserved LV ejection fractions, and thus our finding may not apply to those with abnormal LV ejection fractions. We are unable to quantify the impact of ongoing nitrate, beta-blocker, or calcium-channel blocker use on diagnostic performance.

CONCLUSIONS

QP using stress CMR has higher reproducibility than QA. Quantification of MBF and MPR can detect obCAD more accurately than qualitative analysis performed by CMR experts.

ADDRESS FOR CORRESPONDENCE: Dr Amit R. Patel, University of Virginia Health System, 1215 Lee Street, PO Box 800158, Charlottesville, Virginia 22908, USA. E-mail: apatel@virginia.edu.

PERSPECTIVES

COMPETENCY IN MEDICAL KNOWLEDGE: Absolute sMBF and MPR quantified using vasodilator CMR improve the diagnostic accuracy of obCAD compared with visual assessment.

TRANSLATIONAL OUTLOOK: Quantification of MBF can help standardize interpretation of stress CMR. This has the potential to increase access to stress CMR to less experienced centers without compromising diagnostic accuracy.

REFERENCES

1. Patel AR, Salerno M, Kwong RY, Singh A, Heydari B, Kramer CM. Stress cardiac magnetic resonance myocardial perfusion imaging: JACC review topic of the week. *J Am Coll Cardiol*. 2021;78:1655–1668.

2. Ge Y, Pandya A, Steel K, et al. Cost-effectiveness analysis of stress cardiovascular magnetic resonance imaging for stable chest pain syndromes. *JACC Cardiovasc Imaging*. 2020;13:1505–1517.

3. Nagel E, Greenwood JP, McCann GP, et al. Magnetic resonance perfusion or fractional flow reserve in coronary disease. *N Engl J Med*. 2019;380:2418–2428.

4. Kwong RY, Ge Y, Steel K, et al. Cardiac magnetic resonance stress perfusion imaging for evaluation of patients with chest pain. *J Am Coll Cardiol*. 2019;74:1741–1755.

5. Patel AR, Kramer CM. Quantitative myocardial blood flow assessment using stress cardiac magnetic resonance: one step closer to widespread clinical adoption. *Eur Heart J Cardiovasc Imaging*. 2023;24(4):435–436.

6. Hsu LY, Jacobs M, Benovoy M, et al. Diagnostic performance of fully automated pixel-wise quantitative myocardial perfusion imaging by cardiovascular magnetic resonance. *JACC Cardiovasc Imaging*. 2018;11:697–707.

7. Kotecha T, Martinez-Naharro A, Boldrini M, et al. Automated pixel-wise quantitative myocardial perfusion mapping by CMR to detect obstructive coronary artery disease and coronary microvascular dysfunction: validation against invasive coronary physiology. *JACC Cardiovasc Imaging*. 2019;12:1958–1969.

8. Kotecha T, Chacko L, Chehab O, et al. Assessment of multivessel coronary artery disease using cardiovascular magnetic resonance pixelwise quantitative perfusion mapping. *JACC Cardiovasc Imaging*. 2020;13:2546–2557.

9. Patel AR, Antkowiak PF, Nandalur KR, et al. Assessment of advanced coronary artery disease: Advantages of quantitative cardiac magnetic resonance perfusion analysis. *J Am Coll Cardiol*. 2010;56:561–569.

10. Biglands JD, Ibraheem M, Magee DR, Radjenovic A, Plein S, Greenwood JP. Quantitative myocardial perfusion imaging versus visual analysis in diagnosing myocardial ischemia: a CE-MARC substudy. *JACC Cardiovasc Imaging*. 2018;11:711–718.

11. Benovoy M, Jacobs M, Cheriet F, Dahdah N, Arai AE, Hsu L-Y. Robust universal nonrigid motion correction framework for first-pass cardiac MR perfusion imaging. *J Magn Reson Imaging*. 2017;46:1060–1072.

12. Miller CA, Hsu LY, Ta A, Conn H, Winkler S, Arai AE. Quantitative pixel-wise measurement of myocardial blood flow: the impact of surface coil-related field inhomogeneity and a comparison of methods for its correction. *J Cardiovasc Magn Reson*. 2015;17(1):11.

13. Hsu L-Y, Groves DW, Aletras AH, Kellman P, Arai AE. A quantitative pixel-wise measurement of myocardial blood flow by contrast-enhanced first-pass CMR perfusion imaging: microsphere validation in dogs and feasibility study in humans. *JACC Cardiovasc Imaging*. 2012;5:154–166.

14. Kellman P, Hansen MS, Nielles-Vallespin S, et al. Myocardial perfusion cardiovascular magnetic resonance: optimized dual sequence and reconstruction for quantification. *J Cardiovasc Magn Reson*. 2017;19:43.

KEY WORDS obstructive coronary artery disease, quantitative perfusion, stress cardiovascular magnetic resonance

APPENDIX For an expanded Methods section as well as supplemental figures and tables, please see the online version of this paper.
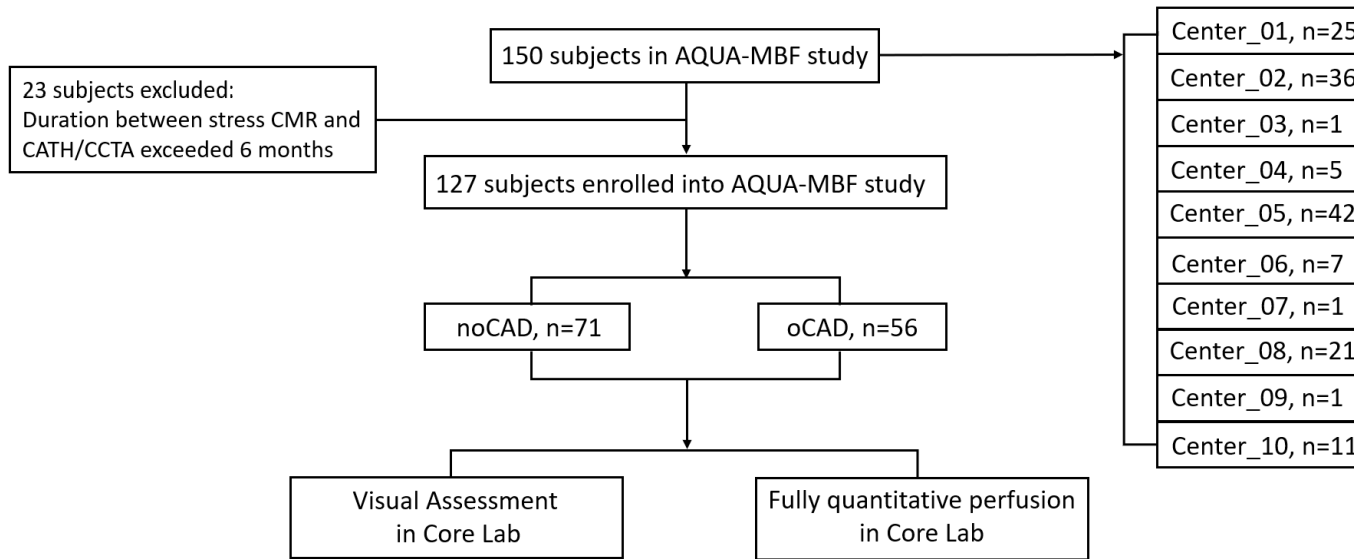
Supplemental Figure 1. The consort diagram for AQUA-MBF study.

Center_01: University of California; Center_02: University of Chicago; Center_03: Stanford University; Center_04: McGill University Health Centre; Center_05: Centro Cardiologico Monzino IRCCS; Center_06: Hospital Universitario Quironsalud; Center_07: Ascires Biomedical Group; Center_08: University of Hong Kong; Center_09: University Hospital Zurich; Center_10: Aarhus University Hospital

A) Global minimum.sMBF decreasing 0.25 ml/g/min

Exposure Group		OR (95% CI)	Interaction p value
Age, years			
<50 (n=24)		2.5 (1.2, 15)	0.854
>=50 (n=102)		2.3 (1.7, 3.3)	
Obese			
No (n=104)		2.3 (1.8, 3.4)	0.754
Yes (n=23)		2.1 (1.3, 4.4)	
Gender			
Female (n=42)		1.9 (1.3, 3.3)	0.532
Male (n=84)		2.3 (1.7, 3.4)	
Diabetes Mellitus			
No (n=80)		2.2 (1.7, 3.3)	0.752
Yes (n=46)		2.5 (1.6, 4.4)	
Hypertension			
No (n=41)		4.5 (2, 20.6)	0.152
Yes (n=85)		2 (1.5, 2.8)	
Hyperlipidemia			
No (n=43)		4.8 (2.2, 18.2)	0.089
Yes (n=83)		1.9 (1.5, 2.7)	
Smoking History			
No (n=98)		2.4 (1.8, 3.4)	0.673
Yes (n=28)		2.1 (1.3, 4.1)	

0.5 2.0
Odds Ratio of obCAD

B) Global minimum.sMBF decreasing 0.25 ml/g/min

Exposure Group		OR (95% CI)	Interaction p value
Scanner			
1.5T (n=82)		2.2 (1.7, 3.3)	0.488
3.0T (n=45)		2.9 (1.7, 6)	
Vasodilator			
Adenosine (n=36)		3.1 (1.7, 8.3)	0.447
Regadenoson (n=91)		2.3 (1.7, 3.3)	
Contrast			
High Relaxivity (n=21)		1.9 (0.8, 7.2)	0.765
Low Relaxivity (n=106)		2.3 (1.7, 3.2)	
Order of Sequence			
Stress First (n=89)		2.1 (1.6, 3)	0.518
Rest First (n=38)		2.7 (1.6, 6.2)	
Cardiac Motion			
No (n=115)		2.6 (1.9, 3.8)	0.035
Yes (n=12)		1.1 (0.5, 2.4)	
2RR acquisition			
No (n=101)		2.4 (1.8, 3.5)	0.901
Yes (n=26)		2.3 (1.3, 5.5)	

0.5 2.0
Odds Ratio of obCAD

C) Global minimum.MPR decreasing 0.25

Exposure Group		OR (95% CI)	Interaction p value
Age, years			
<50 (n=24)		3.6 (1.2, 86.2)	0.558
>=50 (n=102)		2.1 (1.6, 3)	
Obese			
No (n=104)		2.1 (1.6, 3.1)	0.66
Yes (n=23)		2.7 (1.4, 9)	
Gender			
Female (n=42)		1.5 (1.1, 2.5)	0.05
Male (n=84)		2.9 (1.9, 5.1)	
Diabetes Mellitus			
No (n=80)		2.4 (1.7, 3.8)	0.98
Yes (n=46)		2.4 (1.5, 4.6)	
Hypertension			
No (n=41)		3.1 (1.8, 8)	0.275
Yes (n=85)		2 (1.5, 3)	
Hyperlipidemia			
No (n=43)		1.9 (1.3, 3.5)	0.487
Yes (n=83)		2.4 (1.7, 3.7)	
Smoking History			
No (n=98)		2.1 (1.6, 3.1)	0.556
Yes (n=28)		2.8 (1.4, 7.7)	

0.5 2.0
Odds Ratio of obCAD

D) Global minimum.MPR decreasing 0.25

Exposure Group		OR (95% CI)	Interaction p value
Scanner			
1.5T (n=82)		2.4 (1.7, 3.6)	0.832
3.0T (n=45)		2.2 (1.3, 4.3)	
Vasodilator			
Adenosine (n=36)		3.7 (1.7, 12.3)	0.249
Regadenoson (n=91)		2.1 (1.6, 3)	
Contrast			
High Relaxivity (n=21)		1.7 (0.5, 12.7)	0.746
Low Relaxivity (n=106)		2.2 (1.7, 3.2)	
Order of Sequence			
Stress First (n=89)		1.9 (1.4, 2.6)	0.302
Rest First (n=38)		226611.4	
Cardiac Motion			
No (n=115)		2.3 (1.7, 3.3)	0.403
Yes (n=12)		1.6 (0.8, 4.3)	
2RR acquisition			
No (n=101)		2.4 (1.7, 3.6)	0.919
Yes (n=26)		2.5 (1.4, 6.1)	

0.5 2.0
Odds Ratio of obCAD

Supplemental Figure 2. Effect modification of the association between global $_{min}$MBF and obCAD at the patient level. A) global $_{min}$stress MBF and obCAD for different clinical variables. Multivariable logistic regression analyses on effect modification of association between global $_{min}$stress MBF and obCAD in patient level. A, the increased odds ratio (OR) for obCAD in parallel with decreased 0.25ml/g/min of global $_{min}$stress MBF present no significant difference in cardiovascular risks subgroups. B) the increased

odds ratio (OR) for obCAD in parallel with decreased 0.25ml/g/min of global $_{min}$stress MBF present no significant difference in stress CMR technique subgroups except for cardiac motion (interaction P value= 0.035). C) global $_{min}$MPR and obCAD for different clinical variables. The increased odds ratio (OR) for obstructive CAD in parallel with decreased 0.25 of global $_{min}$MPR present no significant difference in cardiovascular risks subgroups D) global $_{min}$MPR and obCAD for different technical variables. The OR for obstructive CAD in parallel with decreased 0.25 of global $_{min}$MPR present no significant difference in subgroups of scanner, vasodilator, 2RR acquisition. Rest first sequence shows the highest OR for obstructive CAD.
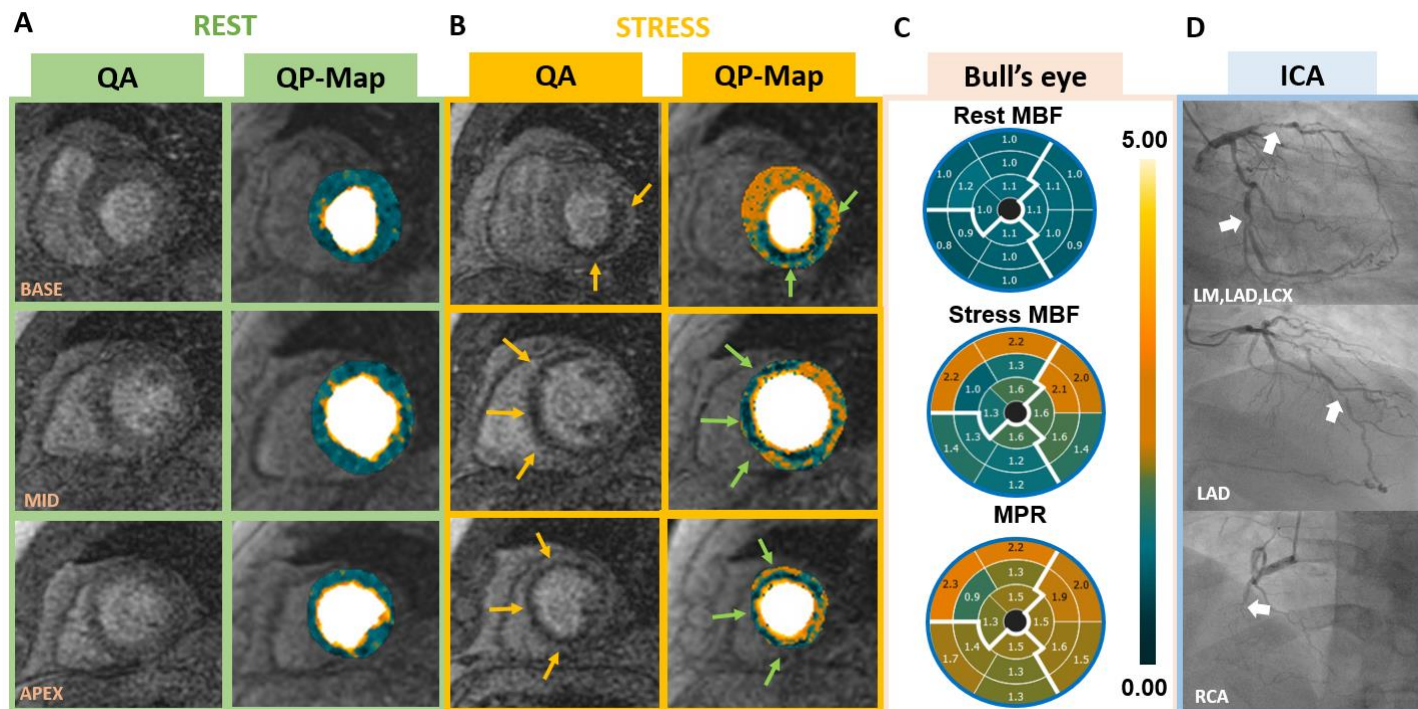
Supplemental Figure 3. Example of obstructive coronary artery disease.

Panels A and B show perfusion images and the corresponding myocardial blood flow (MBF) map during resting and stress conditions. Panel C shows the segmental MBF and myocardial perfusion reserve (MPR) values. Panel D shows the corresponding invasive coronary angiogram findings. The patient has extensive vasodilator induced perfusion defects (see yellow arrows) associated with abnormal pixel-wise perfusion map (see green arrows), reduce stress MBF (<2.04ml/g/min) and MPR values (<1.6) due to multivessel coronary artery disease (see white arrows).

QA – qualitative assessment; QP – quantitative perfusion; ICA – invasive coronary angiography; LM - left main; LAD - left anterior descending; LCX – left circumflex; RCA - right coronary artery.

Supplemental Table 1. Comparison of rMBF, sMBF and MPR between two QP readers at the patient level and at the vessel level.

	Patient level					
	Global$_{mean}$rMBF(ml/g/min)		Global$_{mean}$sMBF(ml/g/min)		Global$_{mean}$MPR	
	noCAD(n=71)	obCAD(n=56)	noCAD(n=71)	obCAD(n=56)	noCAD(n=71)	obCAD(n=56)
QP1	1.00 (0.86, 1.15)	1.05 (0.91, 1.18)	2.38 (2.13, 2.74)	1.53 (1.21, 1.78)	2.05 (1.64, 2.71)	1.31 (1.01, 1.55)
QP2	0.99 (0.86, 1.13)	1.07 (0.91, 1.19)	2.45 (2.13, 2.85)	1.50 (1.17, 1.91)	2.15 (1.69, 2.74)	1.26 (1.02, 1.62)
	Vessel level					
	rMBF(ml/g/min)		sMBF(ml/g/min)		MPR	
	noCAD(n=278)	obCAD(n=103)	noCAD(n=278)	obCAD(n=103)	noCAD(n=278)	obCAD(n=103)
QP1	1.00 (0.90, 1.14)	1.01 (0.90,1.17)	2.25 (1.85, 2.65)	1.45 (1.12, 1.78)	1.90 (1.43, 2.41)	1.20 (0.93, 1.53)
QP2	1.00 (0.88, 1.15)	1.04 (0.91,1.21))	2.26 (1.85, 2.72)	1.52 (1.12, 1.95)	1.92 (1.41, 2.48)	1.27 (0.94, 1.64)

	rMBF(ml/g/min)			sMBF(ml/g/min)			MPR		
	Stenosis <50% (n=258)	Stenosis 50-69% (n=20)	Stenosis ≥70% (n=103)	Stenosis <50% (n=258)	Stenosis 50-69% (n=20)	Stenosis ≥70% (n=103)	Stenosis<50% (n=258)	Stenosis 50-69% (n=20)	Stenosis ≥70% (n=103)
QP1	1.00 (0.90, 1.14)	1.02 (0.91, 1.11)	1.01 (0.90,1.17)	2.28 (1.90, 2.68)	1.51 (1.30, 2.14)	1.45 (1.12, 1.78)	1.94 (1.47, 2.56)	1.39 (1.11, 1.75)	1.20 (0.93, 1.53)
QP2	0.99 (0.87, 1.14)	1.06 (0.96, 1.19)	1.04 (0.91,1.21)	2.29 (1.90, 2.75)	1.61 (1.29, 2.24)	1.52 (1.12, 1.95)	1.94 (1.45, 2.54)	1.32 (1.12, 1.67)	1.27 (0.94, 1.64)

Data are represented as median (Interquartile range). QP1: quantitative perfusion reader1, QP2: quantitative perfusion reader2, rMBF – rest myocardial blood flow; sMBF – stress myocardial blood flow; MPR – myocardial perfusion reserve; noCAD – no obstructive coronary artery disease; obCAD – obstructive coronary artery disease. a: compared to QP1, $p<0.05$. No significant difference of rMBF, sMBF, and MPR are observed between two QP readers.
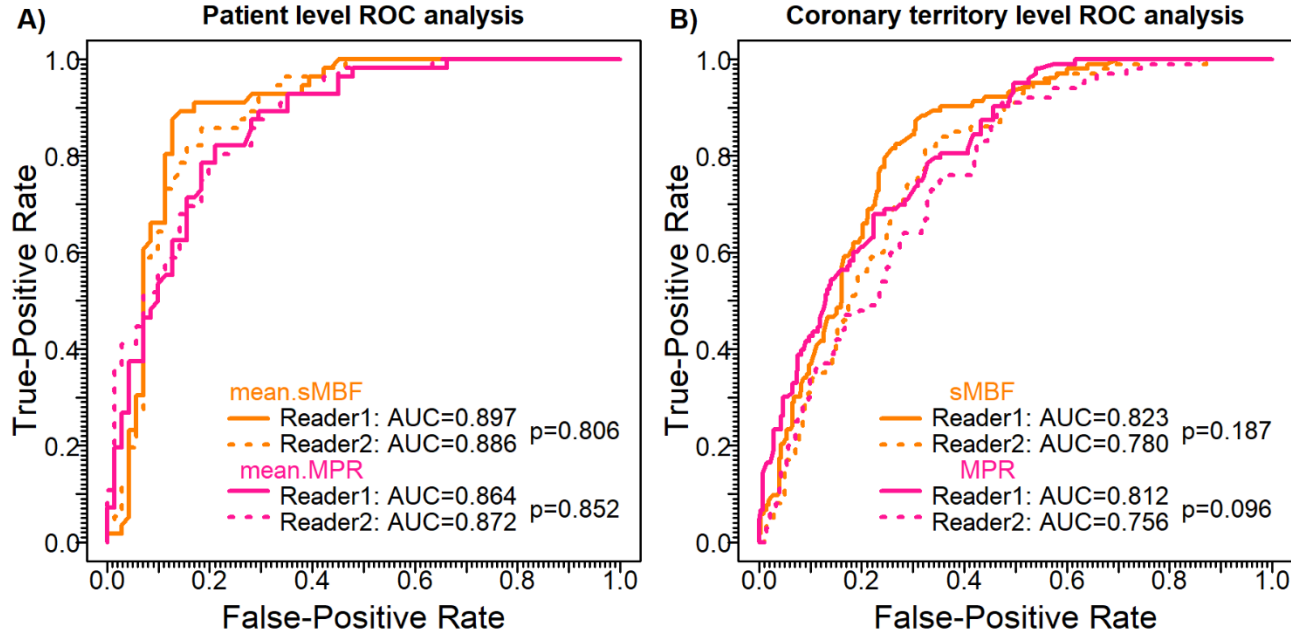
Supplemental Figure 4. Diagnostic performance of QP between two QP readers.

ROC curve for global $_{mean}$sMBF and $_{mean}$MPR for detection of obCAD between two QP readers at the patient level (A). For QP reader1, ROC analysis showed global $_{mean}$sMBF and $_{mean}$MPR had AUCs of 0.90 (95% CI 0.84, 0.96) and 0.86 (95% CI 0.80, 0.93). For QP reader2, ROC analysis showed global $_{mean}$sMBF and $_{mean}$MPR had AUCs of 0.89 (95% CI 0.83, 0.95) and 0.87 (95% CI 0.81, 0.93). There was no significant difference in ROC for sMBF and MPR between two QP readers at the per-patient level ($_{mean}$sMBF: 0.90 vs 0.89, p = 0.806, $_{mean}$MPR: 0.86 vs 0.87, p =0.852).

ROC curve for sMBF and MPR for detection of obCAD between two QP readers at the vessel level (B), for QP reader1, sMBF and MPR had AUCs of 0.82 (95% CI 0.78, 0.87) and 0.81 (95% CI 0.77, 0.86), respectively. For reader 2, sMBF and MPR had AUCs of 0.78 (95% CI 0.74, 0.83) and 0.76 (95% CI 0.71, 0.81). There was no significant difference in ROC for sMBF and MPR between two QP readers at the per-vessel level (sMBF: 0.82 vs 0.78, p = 0.187, MPR: 0.81 vs 0.76, p =0.096).

QP = quantitative perfusion; ROC = receiver operating characteristic curve; sMBF = stress myocardial blood flow; MPR = myocardial perfusion reserve; CAD = coronary artery disease; AUC = area under the curve.

Supplemental Methods

Segmental level

Definition of obstructive coronary disease for the segmental level:

At the segmental level, each segment was categorized as being supplied by a coronary artery with <50% stenosis, 50-69% stenosis, ≥70% stenosis, or presence of LGE in an infarct pattern.

Results.

At the segmental level, sMBF and MPR were significantly lower in LGE segments compared to other non-LGE segments. Similar to the coronary artery level analysis, no statistical difference was observed of sMBF and MPR between segments with 50-69% stenosis and ≥70% stenosis; however, both were lower than segments supplied by <50% stenosis. (**Supplemental Table 2**).

For the segmental level, the distribution of sMBF and MPR by stenosis groups was shown in (**Supplemental Figure 5**). noCAD segments had higher sMBF and MPR values than the CAD segments. The estimated restricted cubic spline function revealed that as the sMBF became greater than 1.7, the likelihood of a segment being supplied by obCAD decreased logarithmically (**Supplemental Figure 6**).

Discussion.

In the segmental analysis of our study, we did not observe a significant difference in stress MBF between segments supplied by a 50-69% stenosis and a ≥70% stenosis. This may reflect the fact that we used the 16-segment AHA model. Some segments may have been assigned to a coronary artery that was not actually supplying it. This is a known limitation of the AHA model. Additionally, a given segment could in the watershed zone of a severely stenosed coronary artery and

a normal coronary artery, resulting in a calculated segmental MBF value representing a mixture of normal and abnormal values. This would have the effect of decreasing differences in MBF values between different segments.
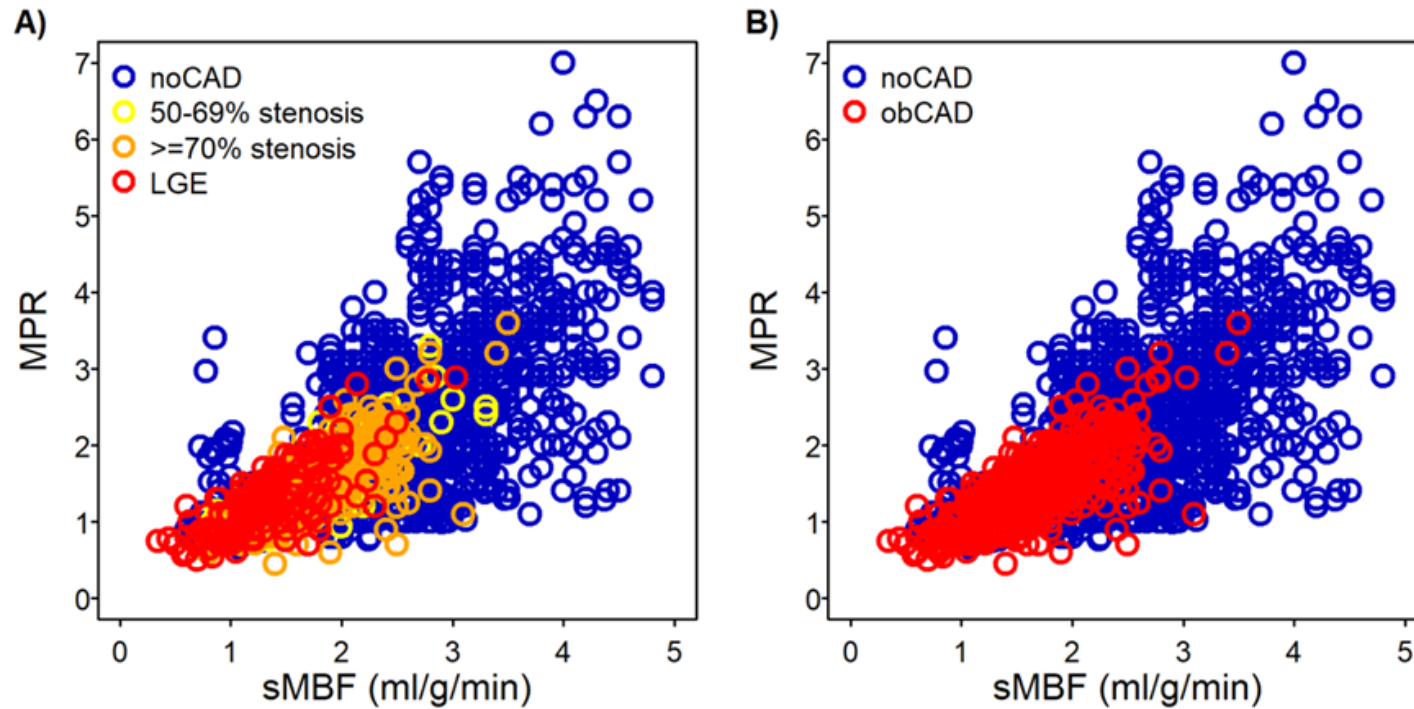
Supplemental Table 2. Comparison of rMBF, sMBF and MPR between noCAD and obCAD at segment level. Data are represented as median (Interquartile range).

	Segment level				
	Stenosis<50% (n=1226)	Stenosis 50-69% (n=97)	Stenosis≥70% (n=268)	LGE (n=162)	P
rMBF (ml/g/min)	1.10 (0.90, 1.30)	1.09 (0.94,1.30)	1.12 (1.00,1.40) c	1.02 (0.90,1.24)	<0.001
sMBF (ml/g/min)	2.50 (2.00, 3.10) abc	1.64 (1.40, 2.20) c	1.77 (1.40, 2.16) c	1.31 (1.02, 1.70)	<0.001
MPR	2.15 (1.58, 2.90) abc	1.50 (1.22, 1.98) c	1.50 (1.10, 1.85) c	1.23 (0.90, 1.51)	<0.001

rMBF – rest myocardial blood flow; sMBF – stress myocardial blood flow; MPR – myocardial perfusion reserve. Segment level: a: compared to stenosis 50-69%, p<0.05; b: compared to stenosis ≥ 70%, p<0.05; c: compared to LGE, p<0.05.

Supplemental Figure 5. Scatter plot of sMBF and MPR.

Panel A represents more detailed segmental description; whereas, panel B divides segments broadly into noCAD vs obCAD.

sMBF = stress myocardial blood flow; MPR = myocardial perfusion reserve; noCAD - no obstructive coronary artery disease; LGE – late gadolinium enhancement; obCAD – obstructive coronary artery disease
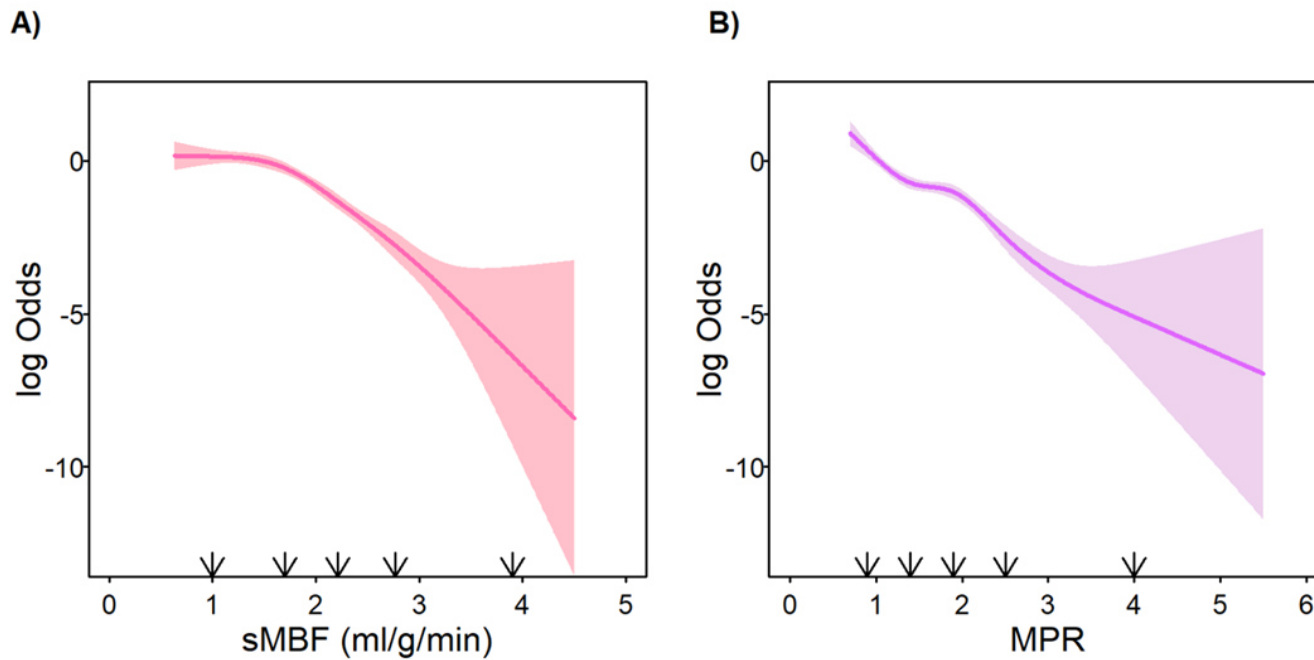
Supplemental Figure 6. Probability of sMBF or MPR is associated with obstructive CAD.

Estimated restricted cubic spline function showing the association between A) sMBF and B) MPR at the segment level and the log odds of obstructive CAD in univariable logistic regression, respectively. The solid line represents the fitted line of the association, and the shaded region represents the 95% CI. The arrows on x-axis show the location of 5 knots which were used in the estimation.

sMBF = stress myocardial blood flow; MPR = myocardial perfusion reserve